

Relation between cyclic deformation mechanisms and mechanical properties in a TiNi shape memory alloy

A-L. Gloanec^a, G. Bilotta^b, M. Gerland^b

a. UME/MS – EnstaParistech – 828 boulevard des Maréchaux – 91762 Palaiseau Cédex (France)

b. Institut P' – Département Physique et Mécanique des Matériaux – UPR3346 – ENSMA – Téléport2 – 1 avenue Clément Ader, BP 40109, 86961 Futuroscope Chasseneuil Cédex (France)

Abstract :

During cyclic loading, the mechanical properties, of a TiNi shape memory alloy, evolve. This evolution is associated with various deformation mechanisms. The objective of this study is to establish a relation between the evolution of the mechanical properties and the implementation of the deformation mechanisms. Three low cycle fatigue tests were performed and stopped at different stages. The first test was stopped after the first cycle. The second was stopped in the 40th cycle, that is the beginning of the stabilization of the cyclic behavior. The last test was performed until failure, which represents 3324 cycles. For each sample, the deformation mechanisms, the transformation temperatures and some mechanical properties, as microhardness, indentation modulus or creep were analyzed. One of the results, which stands out from this study, is that some of the mechanical properties evolve according to the implementation of the deformation mechanisms.

Keywords : Cyclic Stress-Strain Behavior, Shape Memory Alloy, TEM, Mechanical properties

1 Introduction

Shape Memory Alloys (SMA) are widely applied in various industrial fields such as aeronautic (activator ...), biomedical (clips, stents, ...), automotive, civil engineering or domestic (glasses ...) [1, 2]. TiNi alloys are a popular SMA material due to their excellent biocompatibility and mechanical properties, including low weight, good corrosion resistance, and good fatigue strength [3]. SMAs are fascinating materials which present properties that usually do not characterize ordinary metals and alloys. Indeed, TiNi shape memory alloys exhibit very specific thermomechanical behaviors, including shape memory effect [3], good superelasticity [4-6] and high damping capacity at room temperature [7]. Many engineering applications have been developed using some of these properties. Within the frame of design and reliability of systems using SMA, it is essential to have phenomenological models representing thermomechanical behavior. Understanding the physical mechanisms governing the mechanical properties, the cyclic behavior and the failure is a necessary step.

SMA can undergo limited plastic deformation, in a specific temperature range, and then quickly revert back to their original shape, in their high-temperature state, through complete stress relaxation. Such a behavior is called superelasticity, also designated pseudoelasticity. In this paper, this particular behavior is studied.

The objective of this study is to identify the mechanisms governing the mechanical properties during cyclic deformation.

2 Material and Experimental Test Procedures

2.1 Material

A commercial TiNi shape memory alloy containing 51.3% (at.) Ti was used in this investigation. In order to develop pseudoelastic behaviour, a particular thermomechanical treatment was carried out. The various

stages of this thermomechanical treatment were already described elsewhere [8]. The resulting microstructure is then mainly made of fine grains, with an average size of 25 μm [8].

2.2 Test Procedure

The test specimens used were cylindrical with a gauge section of 8 mm in diameter, 20 mm in length and a total length of 120 mm. A mechanical polishing of the gauge length was carried out with silicon carbide paper in order to minimize the effects of the surface irregularities, like work hardening due to machining or oxide layers developed at 850°C, during the first step of the thermo-mechanical treatment. The final surface preparation was then achieved by an electrolytic polishing. Low Cycle Fatigue (LCF) tests were conducted on a servo-hydraulic machine (MTS 810) controlled in force (from 0 to 20.3 kN or 0 MPa to 482 MPa) at 1Hz. In order to work in the austenitic phase, the tests were performed at 50°C. The signal was sinusoidal in shape with a null stress ratio. The strain amplitude was measured by an EPSILON extensometer with a root of 10 mm, placed on the gauge of the test specimen. Three Low-Cycle Fatigue tests were performed and stopped at different stages. The first one was stopped after the first cycle, the second one after 40 cycles, corresponding to the beginning of the CSS behaviour stabilization [4, 8]. The last test was performed until failure ($N_f = 3324$ cycles).

After fatigue tests, samples were cut from the gauge length of the test specimens for Differential Scanning Calorimetry (DSC) measurements, for microhardness tests and for the microstructural characterisation by Transmission Electron Microscopy (TEM).

The cyclic deformation microstructures were examined in a Phillips CM20 transmission electron microscope operating at 200kV [9].

The first step, in characterizing a SMA material, is to determine the characteristic transformation temperatures. There are several transformation temperatures, including the austenite start temperature (A_s), and the austenite finish temperature (A_f) during heating and the martensite start temperature (M_s) and the martensite finish temperature (M_f) during cooling. Additionally, in TiNi SMA, an intermediate phase (R-phase) often appears during cooling, having its own start temperature (R_s) and finish temperature (R_f), before the transformation proceeds to martensite at lower temperature. All these transformation temperatures can be obtained by DSC measurements [10] with a TA DSC Q20 machine. Initially, the material specimen was cooled from approximately 80°C to - 50°C, and then heated from - 50°C to 80°C at 10°C/min. The starting and finishing temperature of each transition phase (M_s , M_f , A_s , A_f , R_s and R_f), the peak temperature (M_p , A_p and R_p) and the heat flow were determined from the DSC thermogram. Note that several cycles of heating and cooling were carried out to be sure that there was not cycling effect on the transformation temperatures.

The microhardness tests were performed on samples polished to 1 μm with a Fischerscope H100C apparatus equipped with a square base pyramidal indenter. Several squares (200 μm x 200 μm) of 49 indentations were done on each sample with a load of 30 mN and a load application time of 15 s. A creep time of 15 s was also added at the maximum load before unloading. The microhardness, the indentation modulus and the creep behavior were obtained for each sample.

3 Results

3.1 Cyclic behavior and deformation mechanisms

The cyclic strain-stress behaviour of a TiNi shape memory alloy is now well known [4, 8, 11]. A classical pseudoelastic response is observed. Contrary to Mouny et al. [4] no residual stress is noticed at the end of the first cycle (Fig.1 – 1 cycle). During cycling, the strain-stress response evolves and reaches a stabilized state. Indeed, the hysteresis loops are modified, changing their form and becoming smaller [8] (Fig.1 – 40 cycles 3324 cycles). Nevertheless, this change tends to stabilize with increasing the number of cycles. This stabilization effect occurs during the first hundred cycles [6]. Here, the stabilization is reached, around 40 cycles.

In previous study, Gloanec et al [9, 12] reported that after the first cycle, the deformation microstructure is characterized by a rather low dislocation density without real interaction between

them. Very thin microtwins, approximately 2 nm or 3 nm in width, can also be seen locally. Almost everywhere a high density of small precipitates can be seen.

After 40 cycles, these authors noted that, the dislocation density is slightly higher but the microtwins are bigger (between 50 nm and 100 nm) and more numerous. Furthermore, they reported the appearance of a new phenomenon: a triple distribution of precipitate size (the first one ranging between 25 and 18 nm, the second one ranging between 16 and 10 nm and the third one between 6 and 2 nm).

After failure, the same authors noticed that, the dislocation density is higher than at low number of cycles, but not very high. Also the density of twins is higher, with sometimes two or even three systems in a grain. Gloanec et al [9] highlighted that, at the same time, the precipitate distribution has evolved towards a non homogeneous configuration with free precipitate channels. The localization of the dislocation activity is probably responsible for the channels empty of precipitates, due to the shearing of precipitates as it has been seen at 40 cycles. Indeed the shearing of a precipitate by several dislocations will induce a size decrease of the precipitate and later its dissolution under its critical size.

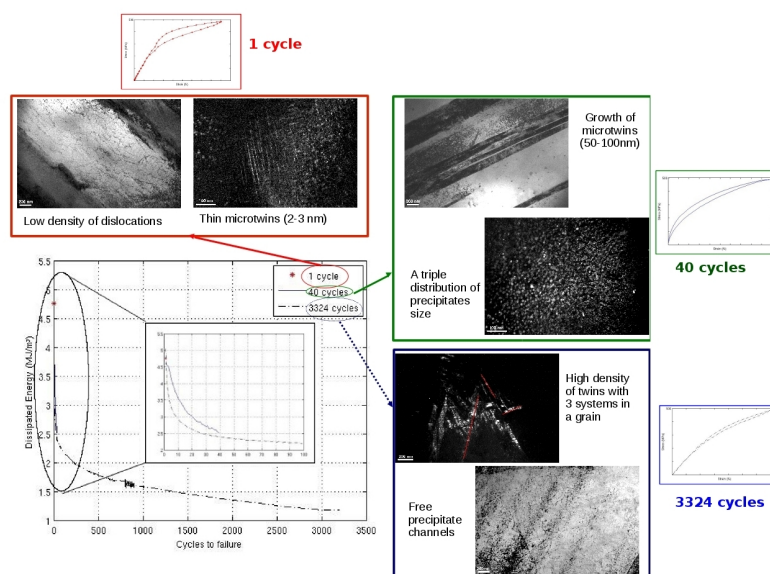


Figure 1 – Cyclic behavior, hysteresis loops and associated microstructures.

3.2 DSC

Transformation temperatures for each cycled sample were reported in the DSC thermogram (heat flow vs. temperature, Figure 2a for tested material and Figure 2b for untested material). For each sample, three heat flow peaks can be observed: a single stage while heating $M \rightarrow A$ transformation and two stages while cooling $A \rightarrow R \rightarrow M$ transformation.

As reported in Figure 2a, the two samples, corresponding to the 1st cycle and to the 40th cycle, present the same behavior during heating and during cooling. Nevertheless, the curve corresponding to 40 cycles is slightly shifted to higher temperatures and the peaks slightly lower in comparison with those of the 1st cycle curve. But now, when the curves of these two samples are superimposed on that corresponding to 3324 cycles, some differences are visible. Indeed, for the peak corresponding to the martensite transformation, the shift towards lower temperature is very marked for 3324 cycles, although it is not the case for the other peaks. The height of the peaks is similar for 1 cycle and 40 cycles but strongly decreases between 40 cycles and 3324 cycles. The areas of the peaks are quite similar for the two first curves (1 and 40 cycles) but much lower for the curve corresponding to 3324 cycles.

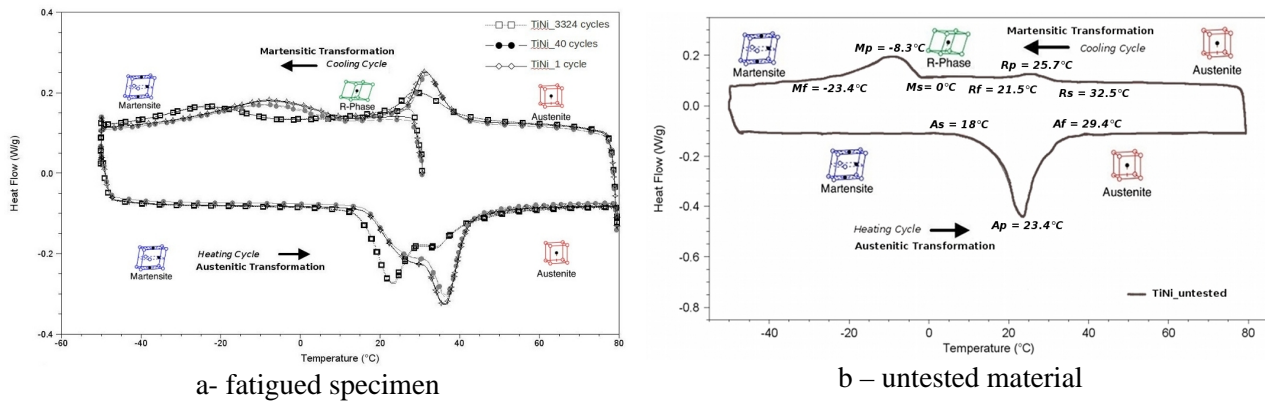


Figure 2 – DSC thermogram.

Just after heat treatment, for the untested material (Fig.2b), a trace of R-phase was observed on the DSC thermogram. The peak of heat flow for this phase, in untested material, is very low regarding the same phase in cycled material.

3.3 Nanomechanical properties

For each sample, six series of 49 indentations were done and the mean values of the microhardness, the indentation modulus and creep are given in the Table 1.

Table1 - Mean values of microhardness, indentation modulus and creep.

	HV (Kg/mm ²)	EIT (GPa)	CIT (%)
1 cycle	438 ± 6	91.8 ± 1.1	3.87 ± 0.15
40 cycles	461 ± 7	95.0 ± 1.0	3.81 ± 0.14
3324 cycles	450 ± 9	89.5 ± 1.5	3.91 ± 0.17

The standard deviation is lower than 2% for the microhardness (HV) which is a rather good result for this material with respect to its microstructure. Regarding its variation during cycling, the microhardness increases by 5.2% between 1 cycle and 40 cycles where it reaches a maximum and slightly decreases by 2.2% between 40 cycles and failure at 3324 cycles.

For the indentation modulus (EIT), the standard deviation is lower than 2%, too. Similarly to the microhardness, the modulus follows the same tendency with variations of 3.5% between 1 cycle and 40 cycles and 5.8% between 40 cycles and failure.

For the creep behavior (CIT), the standard deviation is in the range 3.6% – 4.3%. The creep behavior follows an inverse tendency, firstly a decrease of 1.5% followed by an increase of 2.6%. This tendency is logical.

4 Discussion

A lot of studies [13-17] reveal that temperatures of each transition phase (M_s , M_f , A_s and A_f) and the peak temperatures (M_p and A_p) were influenced by the heat treatment. This study highlights that the presence of the R-phase is also due to cycling. Indeed more the number of cycles is important more the peak of the R-phase is high. As the heat treatment, cyclic loading is now an important parameter which can disturb the phase transformation temperatures and may be at the origin of the intermediate phase (R-phase). Another change is the aspect of the double peak of the austenitic transformation (FIG.2a). For a low number of cycles, the greater peak is situated at a higher temperature while for 3324 cycles it is the contrary, indicating a change in the proportions of the two structures probably associated with the deformation mechanisms observed. Indeed, after 3324 cycles, a non homogeneous configuration with free precipitates channels was observed. This configuration was not detected after the first cycle nor after the 40th.

The evolution of the mechanical properties, like microhardness or indentation modulus and creep, can be expected by an evolution of the microstructure. In this study, contrary to Moumni et al. [4] no residual strain was noticed after the first unloading [8, 9], the material being completely in austenitic phase. Irreversible strain started to appear at the end of the second unloading. That means that after the 40th cycle material was not entirely in austenitic phase, certainly some residual martensite was present. From the first cycle to the 40th cycle, the structure of the material has changed: a small part of the austenitic phase was transformed on residual martensite. This state change imposes a microstructure change [10, 18]. Delobelle et al. [18] demonstrated that indentation modulus increases with grain size. They also noticed that grain orientation has an important influence on the nanomechanical properties. Gloanec et al. [9] reported that the distribution of the indentation sizes (or the hardness values) is not randomly distributed but corresponds to the microstructural characteristics. Jamlech et al. [19] used the same technique to examine the effect of fatigue loading on TiNi. Their results highlighted that the fatigue process revealed a significant decrease in the hardness and elastic modulus of the TiNi. These authors concluded that the fatigue process did not result in work hardening but rather work softening. Indeed, from the first cycle to 3324 cycles (failure of the specimen) our results showed a work softening too. But if result at the 40th cycle is taken into account, the conclusion is then modified. The TiNi shape memory alloy knows a work hardening during the first part of cycling, maybe while the stabilization of the cyclic-strain-stress behavior takes place [6], during 40 cycles in this study. Once the cyclic-stress-strain behavior stabilized, that means no evolution in the shape of hysteresis loops, a work softening can be observed. Another way to explain the evolution of the mechanical properties is the cyclic deformation mechanisms. Gloanec et al. [12] reported that two deformation mechanisms grow simultaneously and without competition: microtwinning and localization of gliding dislocations that shear the precipitates and form channels free of them. The presence of twinning, the production of dislocations and the shear precipitates have already been described by several authors [20-22]. Furthermore Michutta et al. [22] noticed that precipitate size is directly governed by the density of dislocations. Gloanec et al. [12] observed that after failure, the precipitate distribution has evolved towards a non homogeneous configuration with free precipitate channels. The disappearance of precipitates in the channels would predominate on the increase of microtwins to induce a decrease of the nanomechanical properties as the microhardness and the indentation modulus.

5 Conclusion

The objective of this paper was to establish a relation between deformation mechanisms, which appear during low cycle fatigue loading, and the evolution of various mechanical properties, as the microhardness, the indentation modulus or the phase transformation temperatures.

Two results stand out from this study.

The first is that the cyclic loading appears as a new parameter, as important as heat treatment, which can interfere with the phase transformation temperatures and may be at the origin of the intermediate phase (R-phase).

The second is that the implementation of deformation mechanisms, during loading, have an influence on the mechanical properties. Indeed during cyclic loading, until the stabilized state, twins become bigger, and dislocations glide and shear precipitates. These two mechanisms imply a slight increase in the hardness and indentation modulus. Once the cyclic behaviour reaches the stabilized state, a non-homogeneous configuration with free precipitate channels, where dislocations can easily glide, takes place. The implementation of this new configuration leading to a decrease in the nanomechanical properties.

References

- [1] F.E.Feninat, G.Laroche, M.Fiset, D.Mantovani, Shape Memory Materials for Biomedical Applications, *Advanced Engineering Materials* 4 (2002) 91-104.
- [2] C.Boller, Adaptive aerospace structures with smart technologies - a retrospective and future view adaptive structures: engineering applications, M.Friswell (Ed.), 2007.

- [3] K.Otsuka, X.Ren, Recent developments in the research of shape memory alloys, *Intermetallics* 7 (1999) 511-528.
- [4] Z.Moumni, A.Vanherpen, P.Riberty, Fatigue analysis of shape memory alloys: energy approach, *Smart Materials and Structures* 14 (2005) S287-S292.
- [5] S.Nemat-Nasser, W.Guo, Superelastic and cyclic response of NiTi SMA at various strain rates and temperatures, *Mechanics of materials* 38 (2006) 463-474.
- [6] A.Paradis, P.Terriault, V.Brailovski, V.Torra, On the partial recovery of residual strain accumulated during an interrupted cyclic loading of NiTi shape memory alloys, *Smart materials and structures* 17 (2008) 1-11.
- [7] O.Doare, A.Sbarra, C.Touzé, M.Ould Moussa, Z.Moumni, Experimental analysis of the quasi-static and dynamic torsional behaviour of shape memory alloys, *International Journal of Solids and Structure* 49 (2010) 32-42.
- [8] A.L.Gloanec, P.Cerracchio, B.Reynier, A.Vanherpen, P.Riberty, Fatigue crack initiation and propagation of a TiNi shape memory alloy, *Scripta Materialia* 62 (2010) 786-789.
- [9] A.L.Gloanec, G.Bilotta, M.Gerland, Deformation mechanisms in a TiNi shape memory alloy during cyclic loading, *Materials Science and Engineering: A* 564 (2013) 351-358.
- [10] J.A.Shaw, C.B.Churchill, M.A.Iadicola, Tips and tricks for characterizing shape memory alloy Wire: Part1 - Differential Scanning Calorimetry and basic phenomena, *Experimental Techniques* 32 (2008) 55-62.
- [11] C.Dunand-Châtellet, Z.Moumni, Experimental analysis of the fatigue of shape memory alloys through power-law statistics, *International Journal of Fatigue* 36 (2012) 163-170.
- [12] A.L.Gloanec, M.Gerland, Cyclic deformation mechanism in a TiNi shape memory alloy, in: , Proceedings of Low Cycle Fatigue 7, Aachen, Germany, 2013, .
- [13] P.Filip, K.Mazanec, Influence of work hardening and heat treatment on the substructure and deformation behaviour of TiNi shape memory alloys, *Scripta Metallurgica et Materialia* 32 (1995) 1375-1380.
- [14] J.Marquez, T.Slater, F.Sczerzenie. Determining the transformation temperatures of TiNi alloys using differential scanning calorimetry. In . 1997.
- [15] Q.Liu, X.Ma, C.Lin, Y.Wu, Effect of the heat treatment on the damping characteristics of the NiTi shape memory alloy, *Materials Science and Engineering A* 438-440 (2006) 563-566.
- [16] Y.Wang, Y.Zheng, Y.Liu, Effect of short-time direct current heating on phase transformation and superelasticity of Ti-50.8at.%Ni alloy, *Journal of Alloys and Compounds* 477 (2009) 764-767.
- [17] H.Shahmir, M.Nili-Ahmadabadi, F.Naghdi, Superelastic behavior of aged and thermomechanical treated NiTi alloy at Af + 10°C, *Materials and Design* 32 (2011) 365-370.
- [18] P.Delobelle, S.Dali, F.Richard, Interprétation du module d'indentation dans le cas de matériaux anisotropes et/ou actifs, *Matériaux&Techniques* 99 (2011) 185-196.
- [19] A.Jamlech, A.Sadr, N.Nomura, Nano-indentation testing of new and fractured nickel-titanium endodontic instruments, *International Endodontic Journal* 45 (2012) 462-468.
- [20] G.Tan, L.Yinong, P.Sittner, M.Saunders, Lüders-like deformation associated with stress-induced martensitic transformation in NiTi, *Scripta Materialia* 50 (2004) 193-198.
- [21] R.Delville, B.Malard, J.Pilch, P.Sittner, D.Schryvers, Transmission electron microscopy investigation of dislocation slip during superelastic cycling of Ni-Ti wires, *International Journal of Plasticity* 27 (2011) 282-297.
- [22] J.Michutta, M.Carroll, A.Yawny, C.Somsen, K.Neuking, G.Eggeler, Martensitic phase transformation in Ni-rich NiTi single crystals with one family of Ni₄Ti₃ precipitates, *Materials Science Engineering A* 378 (2004) 152-156.